The SIS100 laser cooling facility*

D. Winters[1], T. Beck[2], G. Birkl[‡2], O. Boine-Frankenheim[‡1,2], M. Bussmann[3], L. Eidam[2], V. Hannen[‡4], D. Kiefer[2], S. Klammes[1,2], Th. Kühl[1,5], M. Löser[3,7], X. Ma[§6], U. Schramm[‡3,7], M. Siebold[3], Th. Stöhlker[1,5,8], J. Ullmann[4], Th. Walther[‡2], W. Wen[6], P. Spiller[1]

[1]GSI Helmholtzzentrum, Darmstadt, Germany; [2]Technical University Darmstadt, Germany; [3]Helmholtz-Zentrum Dresden-Rossendorf, Germany; [4]Münster University, Germany; [5]Helmholtz Institute Jena, Germany; [6]Institute of Modern Physics-CAS, Lanzhou, China; [7]Technical University Dresden, Germany; [8]Jena University, Germany

The project group 'SIS100 laser cooling' is setting up a laser cooling facility at the FAIR heavy-ion synchrotron SIS100, being supported by POFIII ARD 'Matter and Technologies'. With the aid of this facility, intense relativistic heavy-ion beams will be laser-cooled to lowest temperatures [1,2]. The project group consists of scientists from GSI and the collaborating partner universities and research centers in Dresden-Rossendorf, Darmstadt, Jena, Münster, and Lanzhou (China).

The laser systems are being developed by the HZDR/TU-Dresden and the TU-Darmstadt, with strong support from the BMBF. These laser systems can be operated at 257 nm or 514 nm, and produce about 100 mW of coherent radiation. The TU-Darmstadt will provide a fast scanning cw-laser system [3], and a pulsed laser system with long (up to 1 ns) pulses and a high repetition rate (up to 1.5 MHz) [4]. The HZDR will provide a pulsed laser system with short pulses (~ps) and a high repetition rate up to 1 MHz [5]. The Münster group will provide an XUV/X-ray detector for the SIS100, again supported by the BMBF [6]. (*Note:* These groups have all applied for a continuation of their funding for the next BMBF period (2018-2021), which shows how committed they are.)

Figure 1: Collage showing a selection of the components purchased in 2017. Upper row: vacuum chamber `mirror box´, rotary fore-pump. Lower row: high-precision wavelength meter, multichannel switch (for 4 laser systems).

In 2017, the design for the laser-detector chamber (LDC) has been completed and a company was selected to manufacture this UHV chamber, the bake-out jackets, and the frame. The chamber is a crucial part of the project: it will be used to couple the laser light into the SIS100 accelerator, and to couple out the fluorescence emitted from the laser-excited ions. The chamber is currently being built by a vacuum company and should be ready in 2018. Also, the design for the first `mirror box´ (vacuum chamber), which an important component of the future SIS100 laser beam line, has been completed. A vacuum company could be found to build and deliver the chamber still in 2017.

In order to be able to test these vacuum chambers (and components inside them), but also for operation later on, vacuum pumps (rotary pump, turbo pump, NEG pump) have been ordered. These pumps are especially quiet and almost without vibrations, so as to prevent for mechanical and acoustical influences on the laser beamline. Since the laser light has to travel via several mirrors over a long distance, small variations in the positions of these mirrors could already lead to noticeable deviations of the laser beam position inside the SIS100 accelerator and modify the overlap between laser and ion beam somewhat.

Since we will have to combine different laser systems at the same time for our experiments at the SIS100, and require very reliable knowledge of the exact wavelengths of these laser systems, a high-precision wavelength meter with a 4-channel switch box is now available for tests and experiments. This way, all laser wavelengths can be measured and monitored as required.

During the year, we have also performed necessary tests of the optical components that are available for the SIS100 laser beam line, such as mirror holders and piezo-actuators. These tests will continue in 2018.

Finally, it seems that it might be possible to perform a laser cooling experiment at the CSRe of the IMP in Lanzhou China in 2018. We are very much looking forward to this important and exciting event. (*Note:* Since the CSRe is rather similar to the ESR, it is very well suited for complementary tests and new experiments.)

References

[1] D. Winters et al., Phys. Scr. **T166** (2015) 014048.
[2] L. Eidam et al., Nucl. Instr. Meth. Phys. Res. A **887** (2018) 102.
[3] T. Beck et al., Opt. Lett. **41** (18) (2016) 4186.
[4] D. Kiefer et al., GSI scientific report 2017.
[5] M. Siebold et al., Opt. Expr. **20** (2012) 21992.
[6] J. Ullmann et al., GSI scientific report 2017.
[7] D. Winters et al., GSI scientific report 2016.

Experiment beamline: none
Experiment collaboration: APPA-SPARC
Experiment proposal: none
Accelerator infrastructure: SIS100
PSP codes: 2.8.10
Grants: *Work supported by HGF POFIII ARD-ST2. ‡Work supported by BMBF. §Work supported by BMBF-WTZ.
Strategic university co-operation with: Darmstadt

Current status of the phase calibration of synchrotron RF reference signals

A. Andreev[1], D. Lens[2], S. Schäfer[2], B. Zipfel[2], D. Domont-Yankulova[1], and H. Klingbeil[1,2]

[1]TEMF, TU Darmstadt, Germany; [2]GSI, Darmstadt, Germany

Introduction

For the successful operation of the FAIR complex it is important to maintain the desired accuracy of the accelerating voltage [1]. The deviation of the phase of the reference signals must not exceed ±1 degree in the whole frequency range from 100 kHz to 6 MHz and a maximum difference of ±3 degrees for the complete system is acceptable. Although closed cavity field control loops stabilize amplitude and phase of the generated RF gap voltages, imperfections of components lead to errors in the signal transmission. Also errors in the detection of the gap voltage affect the accuracy. As a result the actual accelerating voltage interacting with the beam can be different from the target values provided by the Central Control System (CCS). This could compromise reaching the desired beam quality if the above mentioned accuracy requirements are not met. In order to overcome the undesirable errors countermeasures to calibrate synchrotron RF signals are performed.

Group DDS calibration

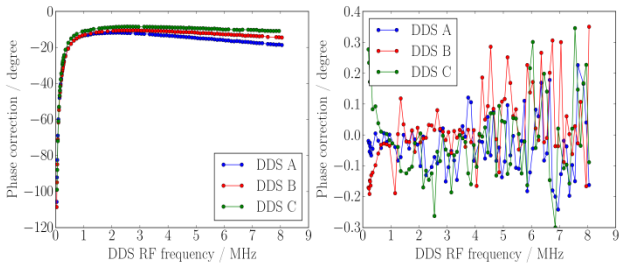

Figure 1: Example for calibration curves of 3 DDS modules before calibration (left) and after calibration (right).

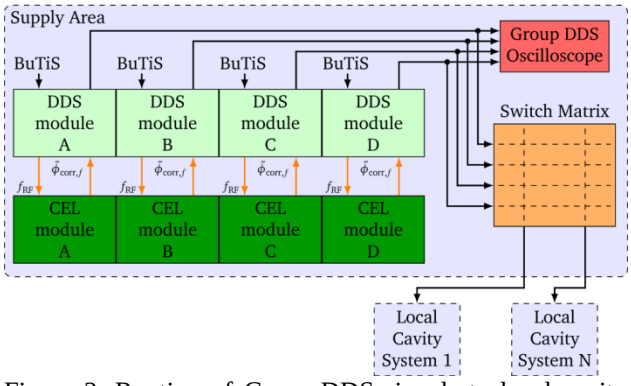

Figure 2: Routing of Group-DDS signals to local cavity systems.

An automated Group DDS phase calibration procedure with respect to the absolute phases of DDS modules defined with BuTiS is described in [2]. Figure 1 shows an example for the calibration curves of modules before and after calibration. It can be seen that the remaining phase response of Group DDS modules is far below 1 degree for the whole frequency range (please note the different scales in the diagrams on the left and on the right), which is within the margins of the phase accuracy requirements. This allows us to conclude that in a supply area it is possible to achieve an in-phase generation of reference RF signals which can later be used for local cavity RF systems (Fig. 2). This also includes the in-phase generation of different harmonics of the revolution frequency, which is needed for example for dual-harmonic operation and bunch merging.

The long term stability of the calibration is important to minimize interruptions needed for accelerator maintenance. First results show that changes of the phase difference between the modules after 3 weeks are within ±1 degree.

Optimisation of parameters

The DDS RF signals' phase accuracy estimation depends on measurement parameters. In order to decrease the deviation of estimated values and increase the precision of the calibration it is important to perform optimisations.

Among the parameters to be optimised are the number of samples per each sinewave and the number of signal periods which are then used to perform a sine wave fit algorithm [3]. Figure 3 shows the first preliminary results for the required number of samples. The next step is the detailed analysis of further parameters and finding their optimal values.

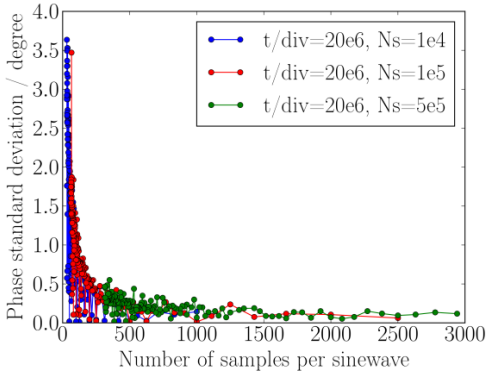

Figure 3: Example for the dependence of the estimated phases' standard deviation on the number of samples per sinewave.

References

[1] H. Klingbeil et al., “New digital low-level rf system for heavy-ion synchrotrons”, Phys. Rev. ST Accel. Beams, vol. 14, p. 102802, 2011.

[2] A. Andreev, H. Klingbeil and D. Lens, “Phase calibration of synchrotron RF signals”, IPAC’17, Copenhagen, May 2017, p. 3945.

[3] P. Händel, “Properties of the IEEE-STD-1057 four-parameter sine wave fit algorithm”, IEEE Trans. on Instr. and Meas., vol. 49, no. 6, pp. 1189-1193, 2000.

 DOI:10.15120/GR-2018-1

Fluorescence detector concept for laser cooling at the SIS100

J. Ullmann[1], V. Hannen[1], D. Winters[2], C. Weinheimer[1]
[1] Westfälische Wilhelms-Universität Münster, Institut für Kernphysik, Münster, Germany
[2]GSI Helmholtzzentrum für Schwerionenforschung Darmstadt, Germany

The acceleration of high intensity ion beams up to the mass range of uranium to highest energies will be possile in the future heavy ion synchrotron SIS100. At Lorentz factors of up to $\gamma = 12$, ion cooling becomes a challenging task and the only feasible option here is laser cooling [1,2]. It requires a fast optical transition in a wavelength region which is accessible to a laser system.

The feasibility of this technique has been demonstrated at lower velocities on C^{3+} ions at the ESR in past beam times [3]. At the high ion velocities expected at SIS100, the energies of the fine structure transition in, e.g., Li-like ions, are blue-shifted by the Doppler effect and allow the application of state-of-the-art UV-laser systems in an anti-collinear setup.

The required counterforce to reduce the momentum spread can not be applied by a co-propagating laser beam, since a laser system producing photon energies in the soft x-ray region is not available yet. The counterforce is therefore exerted by the bucket potential of the bunched ion beam.

To overlap ion and laser beam at one of the six straight sections of the synchrotron, the ion beam is tilted by 2.3 mrad relative to the design orbit and two sets of horizontal and vertical scrapers are used to align both beams. This is schematically shown in Fig. 1.

When the laser frequency is in resonance with the fine structure transition, fluorescence light is emitted isotropically in the ions' rest frame. In the laboratory frame, the emission is transformed by the Lorentz boost to a strongly forward directed cone. Since the cooling takes place at a distance between 12 and 24 meters away from the detector chamber, the angle between ion propagation and detected fluorescence is in the range of 4 to 9 mrad. Here, photon energies in the XUV- and soft x-ray region are expected. A suitable detector requires a sufficient quantum efficiency in this energy range and a high temporal resolution to gain insight to the dynamics of the ion bunch during the cooling process. The spectral resolution of the fluorescence would be even more interesting, since it would allow for spectroscopic measurements of transitions. For many of the medium-heavy Li-like ions, measurements of their fine structure transitions could be performed for the first time here.

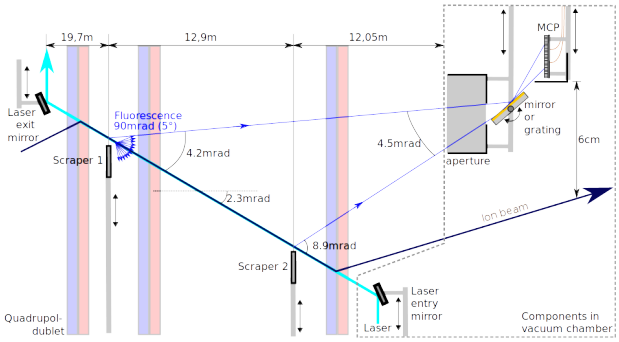

Figure 1: Schematic overview of the proposed detection setup. Ion beam (dark blue) and laser beam (light blue) are overlapped by the use of two scrapers. The fluorescence light (blue arrows) enters the detector chamber at a small angle of few mrad.

The proposed detection setup is schematically shown in Fig. 1 and will be developed in two stages. In the first stage, the timing and the sensitivity of the detector will be optimized. Therefore, a multichannel plate (MCP) detector [4] with a high temporal resolution will be installed. Typical quantum efficiencies of 10% are expected. Estimations of the fluorescence detection rate by a Geant4-simulation are currently ongoing. Enhancements of the efficiency are possible by using a CsI-coated front MCP. An aperture in front of the MCP is used to reduce background light or particles. All parts will be mounted on linear feedthroughs and can be placed at a safe distance from the ion beam during injection and acceleration. Prototypes will be built and tested at Insitut für Kernphysik in Münster.

As a preparation for the second stage, a gold mirror at grazing incidence will be installed on a rotational feedthrough to test the reflection of the fluorescence. Subsequently, the gold mirror will be replaced by a gold coated, laminar flat-field reflection grating with a line density of 2400 lines/mm to diffract the fluorescence light onto the MCP. The planned geometry corresponds to commercially available spectrometers for photon energies of up to 2 keV. Here, a resolving power of 500 is achieved. To detect the spectrum, the MCP will be equipped with a delay-line anode to achieve a spatially resolved detection [4]. An MCP detector with delay-line anode available from the former WITCH experiment at ISOLDE is currently used to equip a new detector test stand in Münster. The data acquisition has been set up and first tests of the read out electronics have been performed.

References

[1] L. Eidam et al., NIM A 887, 102 (2018)
[2] D. Winters et al., this report
[3] D. Winters et al., Phys. Scr. T166, 014048 (2015)
[4] A. Czasch et al., NIM A 580, 1066 (2007)

Experiment beamline: SIS100
Experiment collaboration: APPA-SPARC
Experiment proposal: none
Accelerator infrastructure: SIS100
PSP codes: none
Grants: BMBF 05P15PMFAA
Strategic university co-operation with: none

Tuning rules for the digital filters of the SIS 100 longitudinal feedback system

B. Reichardt[1], J. Adamy[1], D.E.M. Lens[3], D. Domont-Yankulova[1,2], H. Klingbeil[2,3]

[1]TU Darmstadt RMR, Germany; [2]TU Darmstadt TEMF, Germany; [3]GSI, Darmstadt, Germany

Damping of longitudinal coherent bunched-beam oscillations is needed in SIS100 to stabilize the beam, prevent emittance growth and keep beam loss low during acceleration. An FIR (finite impulse response) filter approach with 3 taps, cf. [1], which has already been successfully used at GSI in several machine experiments for beam-phase control in a longitudinal feedback system has further been investigated. The dissertations [2] and [3] deal with an analytical way of how to apply the tuning rules for this approach for stationary, single and dualharmonic operation. In last year's work, extensive tracking simulations were performed to investigate the performance of the feedback system in terms of emittance-growth and settling-time numerically regarding the two tunable parameters of the FIR-filter.

Feedback system

The feedback system can be separated into two parts. One is a bandpass filter, implemented as a symmetric, biasfree bandpass filter. The bandpass frequency, which scales with the linear synchrotron frequency can be detuned by the frequency modificator χ, which is one of the tunable parameters.

The bandpass filtered bunch-phase is integrated and multiplied with a gain factor, to obtain a phase-shift in the gap voltage. The gain-factor also scales with the linear synchrotron frequency. It can further be modified by the gain factor modificator k.

Simulation settings

The tracking simulations have been performed to get a tuning rule for the feedback system, especially for the case of different bunch lengths, synchrotron frequencies and particle energies. Therefore typical synchrotron frequencies for SIS18 (below 2 kHz) and SIS100 (below 1.5 kHz), as well as bunch lengths reaching from 115° to 200° have been tested. The bunch length is the smallest phase range within a bucket, which contains 85% of its particles.

For testing the performance of the filter, the phase of the gap voltage was shifted by 10° to induce a longitudinal dipole oscillation.

Results

In stationary operation constant tuning rules are sufficient. For single harmonic operation the frequency modification factor χ is between 0.95 and 1.0, the gain factor modificator at 0.25. This is comparable to the results for linear buckets in [2].

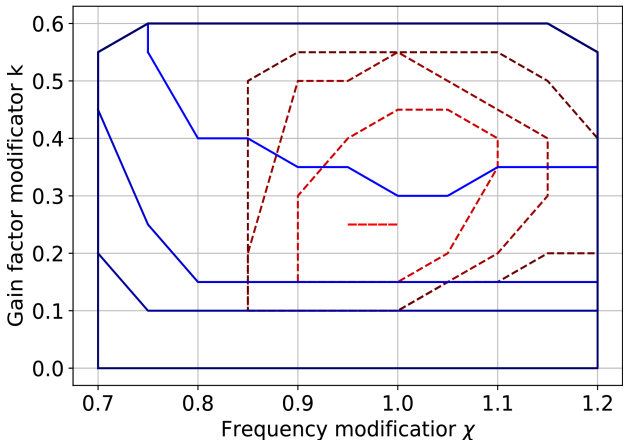

Figure 1: Parameter scan for single-harmonic operation with a bunch-length of 115°. In dashed red are the areas for 2, 3, 4 and 5 oscillations (light to dark) settling time. In solid blue are the areas for 10%, 30%, 50% and 100% (light to dark) relative emittance-growth compared to system without feedback.

For dual-harmonic operation the frequency modification factor is at 0.8 and the gain factor between 0.2 and 0.25. For both parameters, this is about 80% of the parameters used in machine experiments in [3].

In both cases the system is tuned to fast settling times. Notable RMS-emittance-growth from longitudinal dipole oscillations only occurs when the amplitude reaches more than 3 degrees. High damping rates should prevent such critical states.

Outlook

As constant tuning rules for single- and dual-harmonic stationary operation for a large variety of longitudinal beam parameters are sufficient to obtain strong damping rates and decreased RMS-emittance-growth from longitudinal dipole oscillations, it has to be studied whether this also holds on acceleration ramps, due to the strong deformations of the separatrix.

References

[1] H. Klingbeil et al., "A digital beam-phase control system for heavy-ion synchrotrons", IEEE Transactions on Nuclear Science Vol. 54, No. 6, Dec 2007

[2] D. Lens, "Modeling and Control of Longitudinal Single-Bunch Oscillations in Heavy-Ion Synchrotrons", VDI Fortschrittsberichte Vol. 8, No.1209, Düsseldorf, 2012

[3] J. Grieser, “Beam Phase Feedback in a Heavy-Ion Synchrotron with Dual-Harmonic Cavity System”, Dissertation, Darmstadt, 2015

 DOI:10.15120/GR-2018-1

FLUKA/ANSYS study of the APPA beam bump for the BIO-MAT experiment

S. Damjanovic[1], M. Schwickert[1], and V. Venturi[1]

[1]GSI, Darmstadt, Germany

Four beam dumps are planned for the experimental APPA cave, one of which, XBM2SD, will be used for the BIO-MAT experiment (see Figure 1). Given a wide range of different beam parameters (kinetic energies, ion species, time structure) which will be provided for this experiment, multiple FLUKA-ANSYS simulations had to be performed in order to optimize the design of the inner

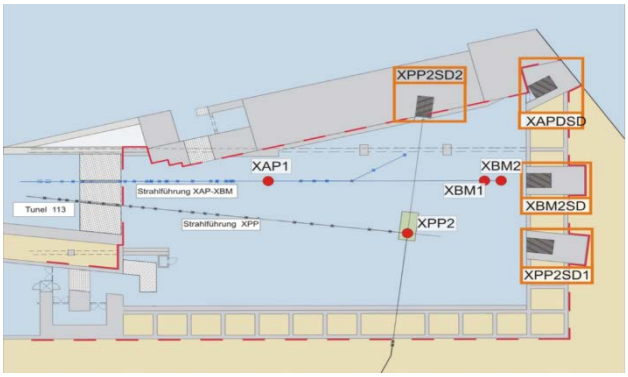

Figure 1: Position of the four beam dumps planned in the experimental APPA cave.

core of the dump as to the dimensions and materials for a safe operation. Another important goal of this study was to find out whether cooling would be required, and if so to propose a cooling design scheme. The starting proposal for the dump core was a composition of a 3m long iron with a 20cm long graphite part at the entrance phase to absorb the Bragg peak region associated with ion beams.

The beams considered for the dump optimization as well as their time structures are summarized in Table 1.

The analysis is based on the following steps. In the first the thermal load from the beam impact is calculated by FLUKA in terms of energy deposition. This is then used as an input into a thermo-mechanical analysis with ANSYS to calculate maximum temperatures and maximum thermal stresses reached by irradiation. After focusing the beam onto the target with a beam radius of 2σx/y=10 mm, the transverse size of the beam at the position of the XBM2SD dump is 2σx/y=30mm.

Table 1: beam parameters considered for the study

Experiment	Particle type	Energy [GeV/n]	Beam Intensity	Time structure
BIO	proton	10	5×1010 /s	Slow extraction
BIO	uranium	10	108 /s	Slow extraction
BIO	carbon	10	108 /s	Slow extraction
BIO	iron	10	108 /s	Slow extraction
MAT	uranium	2	109 /s	Slow extraction
MAT	uranium	0.7	5×1010 /pulse	Fast extraction

For the material risk assessment a thermal-structural analysis was performed. For the highest energy ion beams, the maximum temperatures reached were 29.4 °C for the higher energy uranium beam within the iron part (see Figure 2), and 23 °C for the proton beam within the graphite part, which is about 10 and 100 times lower than the maximum service temperature of iron (230 °C) and graphite (2600 °C), respectively.

The maximum values of the Von-Mises stress were found to be 4.2 MPa within iron part of the dump (see Figure 3) and 1.2 MPa within the graphite part of the dump for the highest energy uranium beam. All values are found to be well below the maximum tensile strengths which are 250 MPa for iron and 30 MPa for graphite of the type R4550.

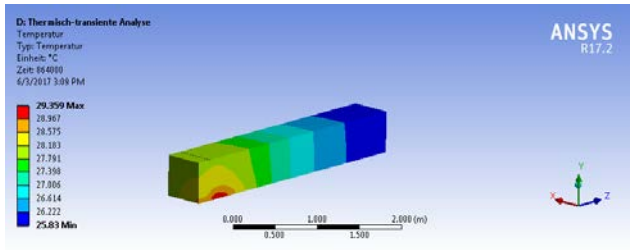

Figure 2: Temperature distribution in steady-state case for a uranium beam at E_k=10 GeV/n

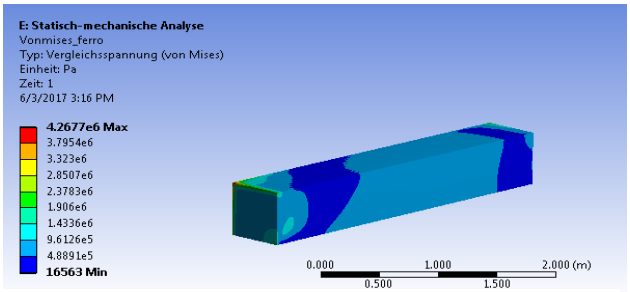

Figure 3: Von-Mises stress distributions for the 3m long iron part of the dump for U beam@E_k=10 GeV/n

Conclusions

The studies presented in this Report indicate that the proposed configuration for the XBM2SD dumps would provide safe operation during the planned running time of the BIO-MAT experiments without any need for active cooling.

FLUKA/ANSYS study of the beam dump for the plasma physics experiment

S. Damjanovic[1], *M. Schwickert*[1], *and V. Venturi*[1]

[1]GSI, Darmstadt, Germany

This report summarizes the concept study for the beam dump XPP2SD1, part of the experimental APPA cave and planned to be used for the Plasma-Physics Experiments. The goal of this study was to optimize the design of the inner cores of the dump as to the dimensions and material, based on coupled FLUKA-ANSYS simulations, which would assure a safe operation. Another important goal of the study was to find out whether cooling would be required. The complete geometry of the APPA cave with the surrounding shielding had already been modelled for the reasons of previous studies related to the optimization of the plasma physics target chamber.

The starting geometry of the XPP2SD1 beam dump was the same as used for the BIO-MAT experiment, i.e.

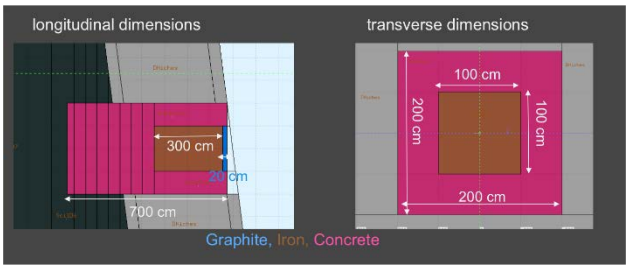

Figure 1: Geometry of the XPP2SD1 beam dump. Side view (left) and cut through the dump (right).

consisting of a 3m long iron core with a 20cm long graphite part at the entrance phase to absorb the Bragg peak region associated with uranium beams (see Figure 1).

The studies are based on an uranium beam intensity of 3×1011 ions/spill at Ek=1 and 2 GeV/n, and on a proton beam of intensity 2.5×1013 p/spill at Ek=5 GeV. A realistic irradiation profile of one pulse every 3 minutes for 10 days is assumed for the analysis. After a strong focusing of the beam onto the target, the beam is very wide at the entrance of the XPP2SD1 dump positioned about 12 m downstream of the target. The transverse beam size at the entrance to the dump is indicated in Table 1.

Beam energy	Beam radius 2σ horizontal size	Beam radius 2σ vertical size
U@2 GeV/n	314 mm	55 mm
U@1 GeV/n	218 mm	126 mm
p@5 GeV	320 mm	320 mm

The analysis steps are the same as used for the studies of the BIO-MAT beam dump. In the first the thermal load from the beam impact is calculated by FLUKA in terms of energy deposition. This is then used as an input into a thermo-mechanical analysis with ANSYS to calculate maximum temperatures and maximum thermal stresses reached by irradiation. The resulting distribution of energydeposition for one pulse of a uranium beam at 2 GeV/n, calculated with FLUKA, is shown in Figure 2 separately for the graphite and iron parts of the inner core of the beam dump.

After considering all three beam configurations, a uranium beam at Ek=2 GeV/n is shown to be the worst-case

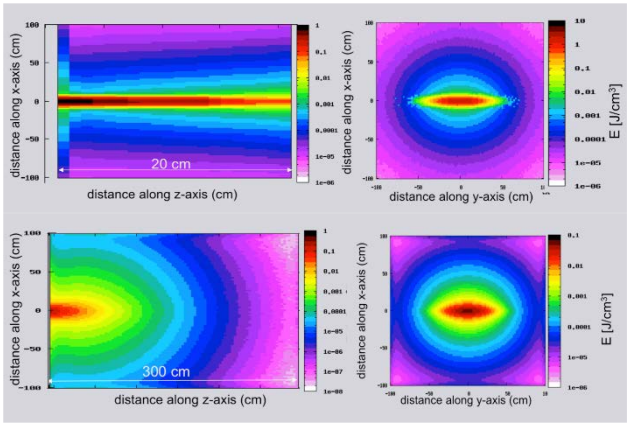

Figure 2: Edep within the core of the beam dump for the C- (upper) and the Fe part (lower) for U@2 GeV/n

scenario. The maximum temperature reached by imposing an average power after 10 days is only 24 ºC on the graphite part. If adding a pulse to the steady state condition, the max T will reach only 27 ºC, far below the maximum service temperature of 2600 ºC for graphite.

The maximum stress reached in each of the pulses is 9 Pa in tension and 0.16 MPa in compression as indicated in

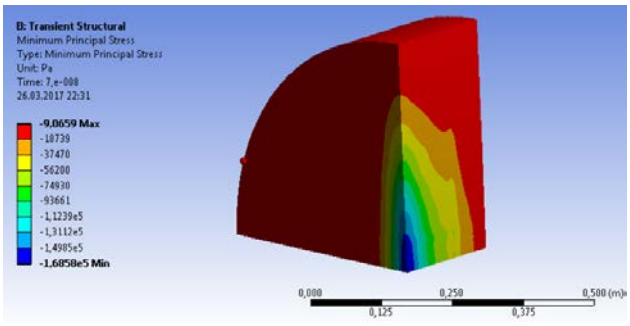

Figure 3: Stress in compression for each of a single uranium 2 GeV pulse.

Figure 3, far from any risk like rapture or yielding.

Conclusions

These results demonstrate that the present configuration of the beam dump will work in safe conditions even for the worst-case scenario and that no active cooling would be required during the whole planned operation including the other beams.

 DOI:10.15120/GR-2018-1

Exploitation of circulant symmetry in SIS18 orbit response matrix

S. H. Mirza[1, 2], H. Klingbeil[1,2], P. Forck[1], R. Singh[1]

[1]GSI, Darmstadt, Germany; [2]TEMF, TU Darmstadt, Germany

Introduction

A closed orbit feedback (COFB) system is under development for the SIS18 synchrotron [1]. This system consists of beam position monitors, a controller and dipolar magnets (correctors). The corrector strength θ_i of each i^{th} corrector (combined in a vector $\boldsymbol{\Theta}$) can be calculated for the position readings y_j of each j^{th} BPM (combined as a vector **Y**) through the inverse of the orbit response matrix (ORM) as given by

$$\Theta = \boldsymbol{R^{-1}Y}. \quad (1)$$

If **R** is not a square matrix, the pseudo-inverse can be used instead of the inverse.

SVD and its relationship with DFT

Singular value decomposition (SVD) is mostly used for the inversion of the ORM [2]. It decomposes a matrix into a product of three matrices, **U**, **S** and **V** where **U** and **V** are orthonormal matrices while **S** is a diagonal matrix of singular values:

$$\mathbf{R} = \mathbf{USV^T} \quad (2)$$

If the matrix is invertible, the inverse is given as

$$\mathbf{R^{-1}} = \mathbf{VS^{-1}U^T}. \quad (3)$$

SVD also helps to calculate the pseudo-inverse ($\mathbf{R^+}$) of non-invertible matrices by providing the liberty to remove smaller or zero singular values in the **S** matrix and their corresponding column of **U** and **V** matrices before inversion.

Decomposed matrices are inter-related with each other; e.g. a unique phase relationship between the columns of **U** and **V** exists. In case of lattice changes during the acceleration ramp, as executed in SIS18, all three matrices need to be recalculated.

Due to the symmetric placement of BPMs and steerers, the vertical ORM of the SIS18 has a special "circulant symmetry" [3]. A circulant matrix can be diagonalized with the help of the discrete Fourier transform (DFT) of only one row or column. The diagonal matrix consists of the complex Fourier coefficients with the standard Fourier matrix **F** as both right and left orthonormal matrix

$$\mathbf{R} = \mathbf{FHF}^*. \quad (4)$$

The DFT-based decomposition of an ORM gives a physical interpretation of SVD modes and a relationship between the two algorithms has been described in the proceeding of ICALEPCS'2017 [4].

Robustness against missing BPMs

Besides the computational benefits of DFT over SVD, sine/cosine DFT modes help to estimate the orbit position at the location of a malfunctioned BPM reading. The idea of modal decomposition is to decompose a perturbed orbit into discrete modes (either SVD or DFT modes) and the elimination of these modes results in a global correction of the orbit. DFT gives a more physical explanation of these modes in the form of pure sine/cosine Fourier modes. These modes can also be used to reconstruct the perturbed orbit by a general curve fitting method. This idea has been employed in this work in order to predict the orbit position at one or two missing BPM locations by fitting the orbit measured with the help of available BPMs over the dominant DFT modes. The CERN accelerator toolbox MAD-X [5] has been used to demonstrate the orbit correction.

Figure 1 shows the perturbed orbit in red and the corrected orbit (when all BPMs are functional) in magenta colours. The black curve shows the scenario when one BPM is missing and there is a significant residual global orbit in the vicinity of the missing BPM after correction using 11 BPMs and 12 correctors. The green curve represents the corrected orbit when the orbit position at the missing BPM location is predicted by DFT fitting (effectively using 12 BPMs with one BPM reading different from actual by the fitting uncertainty). An overall improved correction (lower residual error) is seen in the vicinity of the missing BPM in this case. The blue curve shows a special scenario for comparison when the orbit position is considered to be cantered (0 mm) at the missing BPM location.

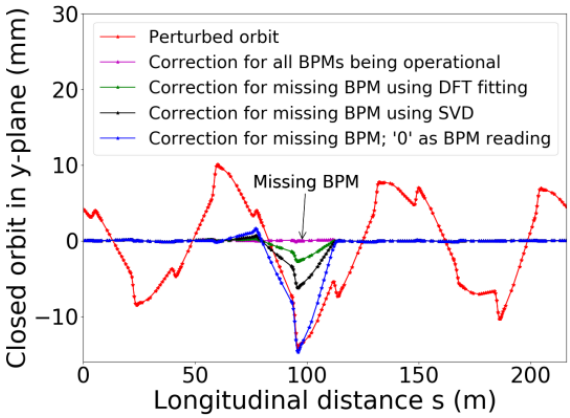

Figure 1: Demonstration of better global orbit correction for missing BPM scenario using estimated orbit position at the missing BPM location.

References

[1] S.H.Mirza, et al. GSI annual report 2017.
[2] Y. Chung *et al.* "Closed orbit correction using SVD of ORM", (Argonne National Laboratory, IL, 1993)
[3] P. J. Davis. "Circulant matrices", Chelsea, 1994.
[4] S.H. Mirza, *et al* Proceedings of ICALEPCS 2017.
[5] http://mad.web.cern.ch/mad/

SIS100 Inspection robot – lane keeping and curved pipes

N. Schweizer[1] and I. Pongrac[2]

[1]TU Darmstadt RMR, Darmstadt, Germany; [2]GSI, Darmstadt, Germany

Current status and steering capability

In previous work we presented a basic robot concept for visual inspection of the SIS100 vacuum system [1,2]. A 3D printed robot prototype was built and it was shown that the robot is able to traverse simple obstacles inside the beamline vacuum system like single steps and gaps. The general robot concept follows a modular design, consisting e.g. of joints between the modules to lift or lower specific parts of the robot. Each module has two driven wheels and all wheels are controlled synchronously. As a result, the robot would only be able to move in a straight direction which has two significant disadvantages.

On the one hand, the robot could leave the center of the beam pipe if initially it is not placed precisely straight or if there are any inaccuracies in the control or manufacturing of the motors. Without steering capabilities the robot would run onto the curved sides of a pipe and would get stuck if the pipe has an elliptical shape, and in cylindrical pipes it could tilt over, which is even worse. On the other hand, the SIS100 is a ring accelerator with curved pipe sections. A robot that moves exclusively straightforward cannot be used here, obviously. Thus, additional joints between the modules must be provided to enable the robot to bend in the horizontal plane.

Description of the new prototype

The problem of steering capabilities and climbing skills can be considered separately. In a first step the joints for vertical movement are neglected. Instead, solely small robot smart actuators are inserted between the modules as it is shown in Fig. 1 for a robot configuration with four modules. The size of these joints is very important because their axles are arranged vertically, and with respect to the dimensions of the SIS100 dipole vacuum chambers the total height of the robot is limited to 5 cm.

According to [3], the velocity of each module must now be controlled separately. To keep the amount of wires manageable, port expanders are placed next to the first and the third joint, respectively. An additional benefit is that only two pins of the microcontroller are needed for an I²C communication with the port expanders instead of 16 to directly control the stepper motors. The servos are interconnected and merely require one control pin. A half duplex asynchronous serial communication enables both write and read instructions. Each servo possesses a unique identification address and can be operated with an angle resolution of 0.29°.

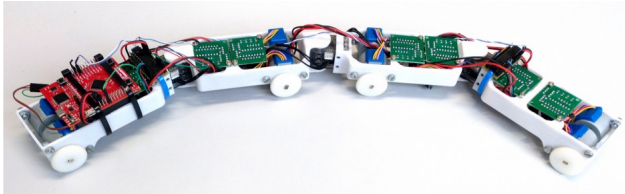

Figure 1: Prototype with four modules and three servos as steering joints.

Further development

Next, the prototype has to be tested and its dynamical parameters must be identified to derive a suitable model which can be used for concurrent simulations and to calculate the steering angles as well as the individual module velocities. With the help of an inertial measurement unit curved pipes or deviations of the robot from the pipe center will be detected and corrected by a dedicated controller.

Currently, a third prototype is under development which combines climbing and steering capabilities in one robot. This is achieved by a series connection of the two different joints between two modules.

Furthermore, the stepper motors will be replaced by robot smart servos, obviating the need for external motor drivers and saving space on the modules, e.g. for essential sensors or batteries. The servos can be set to wheel mode for endless turn. Additionally, the microcontroller board will be substituted with a more sophisticated controller board with smaller dimensions, therefore better fitting into a module.

A major modification will be done for the control concept. To use the same implemented programs as in the robot simulator Gazebo, the robot has to be operated within the Robot Operating System (ROS) framework. For this purpose, the robot will be equipped with a WiFi module to be able to communicate with an external control computer.

References

[1] N. Schweizer and I. Pongrac, IPAC'17, pp. 4528-4530.

[2] N. Schweizer and I. Pongrac, GSI Scientific Report 2016, September 2017.

[3] B. Murugendran et al., IROS'09, pp. 3643-3650.

 DOI:10.15120/GR-2018-1

Commissioning of the beam induced fluorescence monitor for the CERN e-lens

S. Udrea[1], P. Forck[1], M. Ady[2], E. Barrios Diaz[2], O.R. Jones[2], P. Magagnin[2], T. Marriott-Dodington[2], G. Schneider[2], R. Veness[2], A. Salehilashkajani[3], C. Welsch[3], H. Zhang[3]

[1]GSI, Darmstadt, Germany; [2]CERN, Geneva, Switzerland; [3]Cockcroft Institute, Warrington, UK

A hollow electron lens is presently under study as a possible addition to the collimation system for the high luminosity upgrade of the LHC [1], while an electron lens system is also proposed for space charge compensation in the SIS-18 synchrotron for the high intensities at the future FAIR facility. For a precise alignment between the hadron and electron beams a beam diagnostics set-up based on an intersecting gas sheet and the observation of beam-induced fluorescence (BIF) is under development. Its main components are a supersonic gas sheet generator and an intensified camera system. The electron lens will generate a hollow, 5 A, 10 keV electron beam stabilized around the axis of the high energy proton beam by a 4 T solenoidal field. Presently two BIF stations are foreseen, one at each end of the solenoid. There the electron beam is expected to have an outer diameter of ≈10 mm and an inner one of ≈7 mm, while the proton beam will have an rms radius of ≈0.3 mm. The gas sheet is planned to have a width of about 11 mm and a thickness of less than 1 mm. As working gases both N_2 and Ne are considered.

The new BIF monitor set-up

Cross-sections and integration times estimated for both N_2 and Ne [2,3] show that a camera system capable of detecting single photons is required.

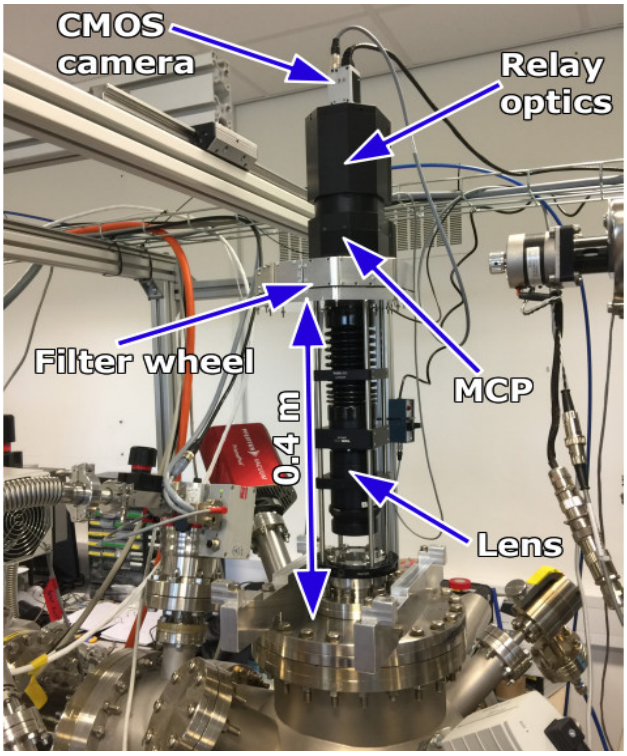

Figure 1: The new BIF set-up as installed at the present gas jet facility at the Cockcroft Institute.

Thus a ProxiKit PKS 2581 TZ-V image intensifier made by ProxiVision and using a Ø 1" double MCP in Chevron configuration has been acquired together with a BASLER acA1920-40gm CMOS camera. The MCP has a UV enhanced S20 photocathode with a quantum efficiency of 5-28% for 260 $< \lambda <$ 650 nm. It can be gated with a minimum gate time of 25 µs and a repetition rate up to 1 kHz. A Schneider Componon 12 35/2.8 lens is used as optical relay to image the phosphor screen on the camera sensor. Several image ratios are possible, e.g. 18:8, 18:11, 25:8, 25:11.

Imaging is achieved with an apochromat lens triplet manufactured by Bernhard Halle Nachfl. GmbH. It is optimised for unit magnification, has an aperture of 40 mm and a focal length of 160 mm. The overall resolution of the optical set-up is 20 lp/mm at magnification 1.2, as assessed with an USAF 1951 test chart. The set-up is shown in Fig. 1.

Results

The measurements at the gas jet facility at the Cockcroft Institute have been performed both with N_2 and Ne as background gases and with a N_2 gas jet. An electron beam generated by a commercial electron gun has been used to excite the gases. Fig. 2 shows the detected interaction between an 30 µA, 5 keV electron beam and an N_2 gas jet.

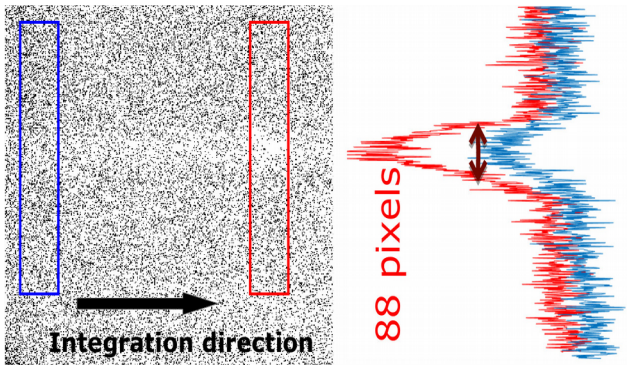

Figure 2: Detected interaction between electron beam and gas jet. The two profiles have been obtained by integration within the marked regions. The increased intensity is due to the gas jet. Images are not to scale.

References

[1] D. Perini and C. Zanoni, arXiv:1702.00234.
[2] S. Udrea et al., IBIC2016, p. 528.
[3] S. Udrea et al., IBIC2017, in press.

Closed orbit feedback system for GSI SIS18 synchrotron

S. H. Mirza[1, 2], A. Bardorfer[3], H. Klingbeil[1, 2], K. Lang, P. Forck[1], P. Kowina[1], R. Singh[1], W. Kaufmann[1]

[1]GSI, Darmstadt, Germany; [2]TEMF, TU Darmstadt, Germany; [3]I-tech Solutions, Slovenia

Introduction

The SIS18 synchrotron will serve as the booster ring for the SIS100 synchrotron of the upcoming FAIR facility to cope with higher beam intensities. One add-on to the existing SIS18 will be a closed orbit feedback (COFB) system for the preservation of the beam quality by stabilizing the beam orbit during the full acceleration cycle. A typical closed orbit feedback system consists of beam position monitors (to measure the orbit), corrector magnets to influence the orbit and a controller built alongside the position monitoring system. The type of controller depends upon many factors e.g. the stability requirements of the closed orbit, temporal responses of the hardware involved in the closed loop, correction bandwidth as well as the requirements on robustness.

The main challenges for the SIS18 COFB are:

1. The thin vacuum chambers (e.g. 0.3 mm for quadrupole chambers) make the beam vulnerable to the power supply ripples as can be seen in figure 1. Also, the fast reaction time during the acceleration ramp (typically lasting 100-500 ms) requires a higher bandwidth of the controller (up to 1 kHz).
2. The change of lattice from triplet to doublet during acceleration ramp resulting in a variable orbit response matrix.
3. Tune movements during the ramp and coherent tune shifts [1].
4. Momentum deviation contributes to the orbit modification during the ramp.

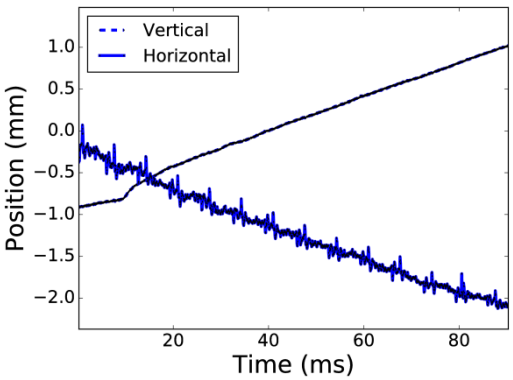

Figure 1: Position in both planes measured at the BPM in section 8 during first 90 ms in the acceleration ramp [2].

Based upon the challenges listed above, a study has been made for the mathematical algorithms used to calculate the corrector strengths in order to find faster and robust algorithms. The details are given in [3].

Hardware preparation

Libera Hadron Platform B is the Slovenian in-kind contribution for the SIS100 COFB which was delivered in January 2018 and is now under test. It will soon be installed at SIS18 and it will also be used as the base-hardware for the SIS18 COFB. It consists of a beam position measurement system based on 16-bit ADCs with a sampling rate of 250 MS/s. A real-time orbit is exchanged between all BPM modules by means of Gigabit data exchange modules (GDX). The GDX modules come inbuilt with a user programmable FPGA where the corrector settings are calculated from the orbit positions grouped from all BPMs at 10 kHz rate. An independent Proportional Integral (PI) controller with an anti-windup protection of each Eigen-mode of the orbit response matrix is also implemented. The magnet settings are then sent to the corrector magnet power supplies via serial interface modules (SER) to the magnet power converters.

The latency of this process is about 30 µs.

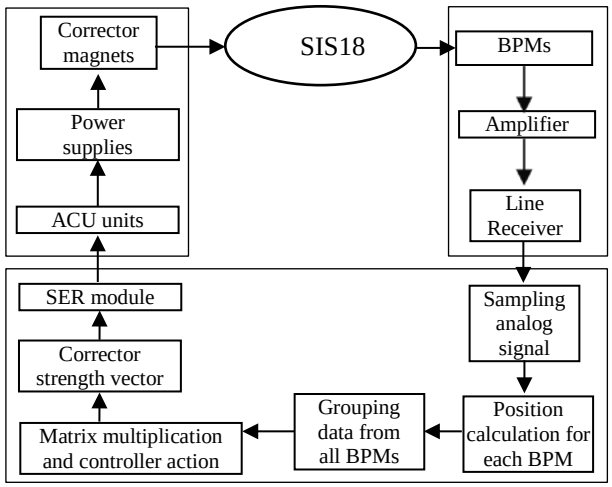

Figure 2: Block diagram of the SIS18 COFB loop

The system identification for the SIS18 COFB loop has been started to estimate the realizable bandwidth. This involves the measurement of transfer functions of corrector magnet power supplies, delay measurements in transmission lines etc. Along with this, the possible model errors and their effects on the closed orbit correction are also being studied through simulations in order to estimate the robustness requirements of the controller. Finally a robust model predictive controller will be implemented on the hardware described above.

References

[1] R. Singh, PhD Thesis, TU Darmstadt
[2] S. H. Mirza, *et al.*, Proceedings of ICALEPCS 2017
[3] S. H. Mirza, *et al.*, Exploitation of circulant symmetry in SIS18 orbit response matrix. In: GSI Scientific Report 2017

 DOI:10.15120/GR-2018-1

Beamloading effects and their influence on cavity detuning in multi-cavity operation in SIS100

D.Mihailescu-Stoica[1], J. Adamy[1], D. Domont-Yankulova[1,2,3], H. Klingbeil[2,3] and D. Lens[3]

[1]TU Darmstadt RMR, Darmstadt, Germany; [2]TU Darmstadt TEMF, Darmstadt, Germany; [3]GSI, Darmstadt, Germany

One possibility to reduce the beam impedance in SIS100 is to detune those cavities that are temporarily unused. Beamloading effects during this detuning are still an open topic. Especially the influence of empty buckets as arising in SIS100 scenarios has to be clarified. We show that the resulting side bands in the beam current limit the degrees of freedom for the impedance reduction strategies.

Critical points during the ramp

Previous results have demonstrated that empty buckets have only a small impact on the beam quality, if only one sum cavity is considered [1]. However, the planned SIS100 heavy ion synchrotron will possess 14 ferrite cavities (20 in the final configuration). Especially during injection and at flat top not all cavities will be active, e.g. during the planned $^{238}U^{28+}$ extreme cycle 18 cavities will be in idle mode during injection and are going to be switched on successively. Up to now the effect of the beam current (including empty buckets) on the induced gap voltage in these idle cavities has not been rigorously investigated. Especially it is an open question if the impedance reduction procedures from SIS18 can be applied unaltered while guaranteeing the desired beam quality.

One of the main approaches besides gap switches is the detuning of the idle cavities to some parking frequencies which are sufficiently separated from the exogenous beam loading disturbance. Anticipating that a single bunch may be sufficiently modelled by a Gaussian distribution during regular operation the corresponding Fourier transform of the beam current is:

$$I_B^{SB}(\omega) = \hat{I}_B \sigma \sqrt{2\pi} e^{\frac{-(\omega\sigma)^2}{2}}$$

The frequency components of the circulating bunch train can be obtained by sampling with a Dirac comb with the frequency $1/T_R$, with $T_R$being the period of revolution. The result is [2]

$$I_B(\omega) = \left(I_B^{SB}(\omega) \sum_{k=1}^{h} \epsilon_k e^{-j\omega k T_{RF}} \right) \sum_{k=-\infty}^{\infty} \delta(\omega - k\omega_R)$$

with σ being the variance of the normal distribution of the particles inside the bucket, h denotes the harmonic number and ϵ_k is parameter equal to 1 or 0 depending on whether the k-th bucket is filled or empty. Figure 1 shows the resulting Fourier coefficients in the cases that eight and ten out of ten buckets are filled with bunches. While in the case that all buckets are filled, only the harmonics appear, the existence of empty buckets leads to considerable sidebands. Consequently, the choice of suitable parking frequencies for the idle cavities is restricted due to the existence of these parasitic components.

Figure 1 shows that for the choice of the resonance frequency of

$$\omega_n = (1/2 + n)\omega_{RF}, \qquad n \in \mathbb{N}_0,$$

the amplitudes of the Fourier coefficients are zero. These frequencies represent natural candidates for detuning of the cavities via the resonance control loop. Due to symmetry, this result also holds during injection, when two buckets are perpetually injected in the synchrotron.

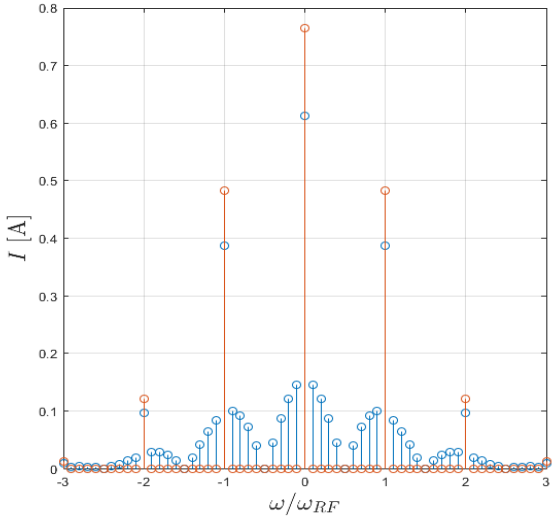

Figure 1: Fourier coefficients of the beam with eight out of ten filled buckets (blue) and Fourier coefficients of the beam with ten out of ten filled buckets (red).

Outlook

For the operation of the SIS100 accelerator with up to 20 ferrite cavities additional investigations are indispensable. Due to the existence of empty buckets, previous impedance reduction strategies from the predecessor SIS18 cannot be directly applied to SIS100. In the case that the cavities will be detuned, extensive simulations will be needed to specify the requirements on the transient detuning dynamics. The assumption underlying this analysis is the Gauss distribution of the particles in the beam. Especially during slow extraction this assumption is not justified. Thus, this case has to be treated separately towards clarifying the question, if impedance reduction via detuning alone suffices to guarantee successful operation.

References

[1] D. Mihailescu-Stoica, J. Adamy, D. Domont-Yankulova, H. Klingbeil and D. Lens, “Behaviour of the planned RF feedback loops under beam loading during a reference SIS100 Cycle”, GSI Scientific Report 2016

[2] D. Mihailescu-Stoica, D. Domont-Yankulova, D. Lens and H. Klingbeil, “On the impact of empty buckets on the ferrite cavity control loop dynamics in high intensity hadron synchrotrons”, IPAC’17, Copenhagen, May 2017.

Signal processing hardware for single-bunch manipulation*

M. Hardieck[†3] *, D. Lens*[‡1] *, K. Groß*[2] *, H. Klingbeil*[1,2] *, M. Kumm*[3] *, and P. Zipf*[3]

[1] GSI; [2] TU Darmstadt, TEMF; [3] University of Kassel, Digital Technology Group

Overview of the System

The bunch-by-bunch longitudinal feedback planned for SIS100 is a broad-band feedback system (BBFB) that will help to stabilize the beam, keeping longitudinal emittance blow-up low and minimizing beam losses [1]. The most components of the system are mainly based on hardware and software components that have already been successfully tested in several machine experiments at SIS18, e.g., [2, 3]. However, new components have to be developed such as a bunch signal de-multiplexer and multiplexer (MUX). The progress on the development of the digital MUX and an overview of its properties is reported in the following.

Multiplexer Prototype

The BBFB system separates the beam current into 10 channels. For each channel (each represents a single bunch) an analog preprocessing unit and a DSP System calculates phase and amplitude correction values and converts them into inphase and quadrature components (I/Q). These signals are used by the MUX to modulate the RF signal for the kicker cavities, which allows individual manipulation for each bunch. [4]

Currently, a system prototype is under test in a laboratory environment at GSI. An example MUX output for harmonic number h=4 is shown in Figure 1. The signals in the upper half are based on the beam (C1 ≙ h=1, C2 ≙ h=4). The lower signal (C3) is the output generated by the MUX. The output is synchronized with the RF signal (h=4) and modulates different outputs for each bunch. The first bunch is set to zero. The second one is not modulated. The third has triple amplitude and the last has twice the amplitude and a phase shift of -90°. The bunch numbering starts every rising edge of the h=1 sine signal (C1).

System Specifications

In Table 1, the primary parameters of the current implementation are shown. The total system latency is the time difference from the RF (sine) input signal which corresponds to the bunch frequency and the analog output of the system. The correction value consist of an I-part and a Q-part. Finally, the whole output signal can be scaled with a relative amplitude. The output signal is generated by a digital to analog converter (DAC) which has 14 bit resolution. It is planned to adapt the design to a newer hardware platform. This would allow a higher clock frequency which leads to smaller bunch transition jitter and less latency.

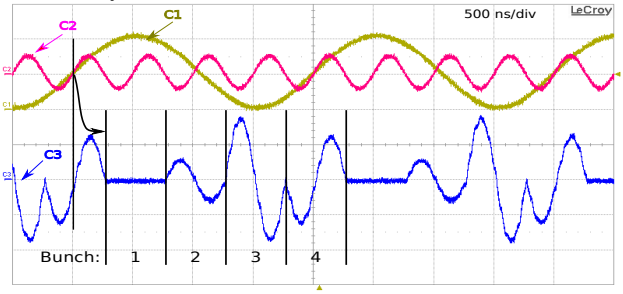

Figure 1: Example MUX output for h=4 (h=1 is 500 kHz)

Table 1: System properties

Parameter	Value
Sampling Frequency	80 MHz
Total System Latency	250 ns
ADC/DAC contribution	112.5 ns
Computation contribution	137.5 ns
Bunch Transition Jitter	25 ns
Q-Range	-3 to +3
Q-Resolution	2^{-13}
I-Range	-3 to +3
I-Resolution	2^{-13}
Relative Amplitude Range	0 to 255
Relative Amplitude Resolution	2^{-24}
Output Signal Resolution	14 bit
Max RF Frequency	5.5 MHz
Max Supported Bunches	16

Outlook

As a next step, a machine experiment with beam at SIS18 using one of the h=2 magnetic alloy cavities as dedicated kicker cavity is planned to evaluate the setup.

References

[1] K. Groß et al., GSI SR 2014, FG-SIS100-10 (2015).
[2] H. Klingbeil et al., “A digital beam-phase control system for heavy-ion synchrotrons”, IEEE Trans. Nucl. Sci. 54(6)2604:2610 (2007).
[3] D. Lens et al., GSI SR 2014, FG-GENERAL-29 (2015).
[4] D. Lens et al., GSI SR 2016, FAIRPROJECT-SIS100-SIS18-15 (2017)

∗ Work supported by GSI.
† hardieck@uni-kassel.de
‡ d.e.m.lens@gsi.de

 DOI:10.15120/GR-2018-1